

Articles

A Theoretical Insight into the Ability of Group 6 ML_5 Metal Fragments to Break the H–H Bond

Jaume Tomàs and Agustí Lledós*

Departament de Química, Universitat Autònoma de Barcelona, 08193 Bellaterra, Spain

Yves Jean*

Laboratoire de Chimie Théorique (URA 506), Bât. 490, Université de Paris Sud,
91405 Orsay Cedex, France

Received April 22, 1998

The interaction between H_2 and $M(CO)_n(PH_3)_{5-n}$ ($M = Cr, Mo, W; n = 0, 3, 5$) metal fragments has been studied by means of CCSD(T)//B3LYP calculations. Three steps in the dihydrogen addition path that starting from the ML_5 and H_2 separated fragments leads to a stable dihydride have been considered: (i) dihydrogen coordination; (ii) cleavage of the H–H bond in a dihydrogen-like structure, leading to a **PB1** *cis*-dihydride; (iii) reorganization of the pentagonal bipyramidal *cis*-dihydride formed to a more stable **PB2** dihydride structure. From the thermodynamic results and the energy profiles for the oxidative addition the nine complexes under study can be classified in three groups: (i) only dihydrogen observable; $M(CO)_5H_2$ ($M = Cr, Mo, W$); and $M(CO)_3(PH_3)_2H_2$ ($M = Cr, Mo$); (ii) equilibrium between dihydrogen and **PB2** dihydride: $W(CO)_3(PH_3)_2H_2$ and $M(PH_3)_5H_2$ ($M = Cr, Mo$); (iii) only dihydride observable; $W(PH_3)_5H_2$. The different behavior for dihydrogen addition is related to the energetics of the M– H_2 and M–H bonds and to the singlet–triplet separation in the ML_5 fragment.

Introduction

The interaction between an H–H bond and a metallic center plays a crucial role in catalytic hydrogenation processes.¹ For a long time it has been thought that this interaction necessarily leads to the H–H bond breaking and to the formation of a dihydride complex, in the so-called oxidative addition process.² Since the discovery in 1984 of a dihydrogen complex,³ in which an H_2 molecule is coordinated to a transition metal fragment, the evidence that such complexes may be intermediates along the pathway for H_2 oxidative addition forced a revisitation of this important class of reactions. The oxidative addition may be achieved either directly or through a two-step mechanism involving first the intermediate formation of a stable dihydrogen complex. In the latter, further breaking of the H–H bond leads to a classical *cis*-dihydride which may reorganize to a more stable dihydride structure. Finally, there are also systems in which the reaction

process cannot go further than the initial stage, the formation of the dihydrogen complex.^{4,5}

Since the first well characterized η^2-H_2 complex was the hexacoordinated $W(CO)_3(P-i-Pr)_2(\eta^2-H_2)$ tungsten complex,³ very special attention was paid recently to the interaction of H_2 with group 6 ML_5 metallic fragments, bringing on a wide variety of experimental data on ML_5H_2 compounds. All the complexes of formula $M(CO)_n(PR_3)_{5-n}H_2$ ($M = Cr, Mo, W; n = 0, 3, 5$) have been synthesized. They offer the opportunity to obtain a clear picture of the factors that govern the way an H_2 molecule interacts with a metallic center. All types of metal– H_2 interactions have been actually found, depending on the nature of the metal and the ancillary ligands. The $M(CO)_3(PR_3)_2H_2$ ^{3,6,7} and $M(CO)_5H_2$ ⁸ com-

(1) James, B. R. *Homogeneous Hydrogenation*; Wiley: New York, 1973. (b) Chaloner, P. A.; Esteruelas, M. A.; Joó, F.; Oro, L. A. *Homogeneous Hydrogenation*; Kluwer Academic Publishers: Boston, MA, 1994.

(2) Collman, J. P.; Hegedus, L. S.; Norton, J. R.; Finke, R. G. *Principles and Applications of Organotransition Metal Chemistry*; University Science Books: Mill Valley, CA, 1987; Chapter 5.

(3) Kubas, G. J.; Ryan, R. R.; Swanson, B. I.; Vergamini, P. J.; Wasserman, H. J. *J. Am. Chem. Soc.* **1984**, *106*, 451.

(4) Kubas, G. J. *Acc. Chem. Res.* **1988**, *21*, 120. (b) Kubas, G. J. *Comments Inorg. Chem.* **1988**, *7*, 17. (c) Crabtree, R. H. *Acc. Chem. Res.* **1990**, *23*, 95. (d) Jessop, P. G.; Morris, R. H. *Coord. Chem. Rev.* **1992**, *121*, 155. (e) Heinekey, D. M.; Oldham, W. J., Jr. *Chem. Rev.* **1993**, *93*, 913.

(5) Crabtree, R. H.; Hamilton, D. G. *Adv. Organomet. Chem.* **1988**, *28*, 299. (b) Crabtree, R. H. *Angew. Chem., Int. Ed. Engl.* **1993**, *32*, 789.

(6) Kubas, G. J.; Ryan, R. R.; Wroblewski, D. A. *J. Am. Chem. Soc.* **1986**, *108*, 1339. (b) Kubas, G. J.; Unkefer, C. J.; Swanson, B. I.; Fukushima, E. *J. Am. Chem. Soc.* **1986**, *108*, 7000. (c) Zilm, K. W.; Millar, J. M. *Adv. Magn. Opt. Reson.* **1990**, *15*, 163.

(7) Kubas, G. J.; Nelson, J. E.; Bryan, J. C.; Eckert, J.; Wisniewski, L.; Zilm, K. *Inorg. Chem.* **1994**, *33*, 2954.

(8) Sweany, R. L. *J. Am. Chem. Soc.* **1985**, *107*, 2374. (b) Upmacis, R. K.; Poliakov, M.; Turner, J. J. *J. Am. Chem. Soc.* **1986**, *108*, 3645.

plexes (M = Cr, Mo, W; R = Cy, *i*-Pr) have been characterized as dihydrogen species, whereas M(P-Me₃)₅H₂ (M = Mo, W)⁹ and M[P(OMe)₃]₅H₂ (M = Cr, Mo, W)¹⁰ complexes have been described as seven-coordinate dihydride molecules.

Theoretical studies have played an important role in the understanding of the nature of dihydrogen–metal bonding.¹¹ In addition, structural properties of η²-H₂ complexes, sometimes hardly accessible from experimental methods, have been calculated with great accuracy.¹² The ligand and metal effects on the relative stabilities of a series of transition metal dihydrogen compounds with respect to their dihydride isomers have also been inferred.^{11,13} The replacement of pure σ-donor ligands as PR₃ by π-acceptor ones as CO weakens the interaction between a d⁶ ML₅ fragment and the H₂ molecule and makes the dihydride formation more difficult because the back-donation toward H₂ is reduced. Changing a third-row metal with high lying d orbitals by a first-row metal with lower lying d orbitals also disfavors the dihydride formation.

Less attention has been devoted to the very process of oxidative addition that interconverts a d⁶ ML₅(η²-H₂) complex into a *cis*-dihydride. In a previous work, we reported the study of the W(CO)₃(PH₃)₂(H₂) used as a model for the Kubas complex, by means of CCSD(T)//B3LYP calculations.¹⁴ In this paper our study is extended to the whole series of M(CO)_n(PH₃)_{5-n}H₂ complexes (M = Cr, Mo, W; *n* = 0, 3, 5) to obtain a thorough picture of the way an H–H bond interacts with a group 6 ML₅ metal fragment all along the pathway for the oxidative addition. The particular behavior of a ML₅ fragment is related through a thermodynamic cycle to its physical properties and to the energetics of M–H₂ and M–H bonding.

Method of Calculation

Calculations were performed with the GAUSSIAN 94 series of programs¹⁵ using the same methodology than in our previous study of the Kubas complex.¹⁴ Geometry optimizations were carried out using the density functional theory (DFT)¹⁶ with the B3LYP functional.¹⁷ An effective core potential operator was used to represent the innermost electrons of the

chromium, molybdenum, and tungsten atoms.¹⁸ The basis set for the metal atoms was that associated with the pseudopotential,¹⁸ with a standard valence double-ζ LANL2DZ contraction.¹⁵ The basis set for the hydrogen atoms directly attached to the metal was a double-ζ supplemented with a polarization p shell.^{19a,b} A 6-31G basis set was used for the other H atoms, as well as for carbon and oxygen atoms.^{20a} The phosphorus atoms were described with the 6-31G(d) basis set.^{19c}

To obtain accurate estimations for the dihydrogen/dihydride relative energies, as well as for the oxidative addition energy profiles, the geometries were optimized at the B3LYP level and the energies recalculated using coupled-cluster theory with single, double, and a noniterative estimation of triple excitations (CCSD(T)//B3LYP).²⁰ This calculational scheme has been proposed to obtain accurate energy values²¹ and has been successfully tested in our previous article. It has recently been proved in several transition metal dihydrogen complexes that a similar approach, based on single-point CCSD(T) calculations on MP2 optimized geometries, gives energetic values in excellent agreement with the experimental data.^{13c} The metal-dihydrogen and metal–hydrogen dissociation energies as well as the singlet/triplet energy differences in the ML₅ fragments were also calculated at the CCSD(T)//B3LYP level.

Dihydrogen Complexes

We began our study of the dihydrogen oxidative addition to group 6 ML₅ fragments looking for the stabilities of the dihydrogen species. We have fully optimized at the B3LYP level the dihydrogen complexes. The optimized M–H and H–H bond lengths are reported in Table 1, together with the H₂ dissociation energies (*D*_e(M–H₂)) computed at the CCSD(T)//B3LYP level. *D*_e(M–H₂) was calculated as the energy difference between the optimized dihydrogen complex and the optimized ML₅ and H₂ fragments. The optimized structures for the three molybdenum compounds are depicted in Figure 1. The first remarkable result is that the dihydrogen species are stable at the B3LYP level for the nine systems under study. Taking as a starting point in the optimization a dihydrogen-like configuration geometry, optimizations lead to structures in which the H–H distance is always shorter than 0.92 Å. However, data reported in Table 1 clearly indicate energetic and structural changes depending on the nature of the metal and the ancillary ligands.

(9) Chiu, K. W.; Jones, R. A.; Wilkinson, G.; Galas, A. M. R.; Hursthouse, M. B.; Abdul Malik, K. M. *J. Chem. Soc., Dalton Trans.* **1981**, 1204. (b) Lyons, D.; Wilkinson, G.; Thornton-Pett, M.; Hursthouse, M. B. *J. Chem. Soc., Dalton Trans.* **1984**, 695.

(10) Choi, H. W.; Gavin, R. M.; Muetterties, E. L. *J. Chem. Soc., Chem. Commun.* **1979**, 1085. (b) Choi, H. W.; Muetterties, E. L. *J. Am. Chem. Soc.* **1982**, *104*, 153. (c) Van Catledge, F. A.; Ittel, S. D.; Jesson, J. P. *Organometallics* **1985**, *4*, 18.

(11) Some theoretical studies: (a) Jean, Y.; Eisenstein, O.; Volatron, F.; Maouche, B.; Sefta, F. *J. Am. Chem. Soc.* **1986**, *108*, 6587. (b) Hay, P. J. *J. Am. Chem. Soc.* **1987**, *109*, 705. (c) Eckert, J.; Kubas, G. J.; Hall, J. H.; Hay, P. J.; Boyle, C. M. *J. Am. Chem. Soc.* **1990**, *112*, 2324. (d) Pacchioni, G. *J. Am. Chem. Soc.* **1990**, *112*, 80. (e) Maseras, F.; Duran, M.; Lledós, A.; Bertrán, J. *J. Am. Chem. Soc.* **1991**, *113*, 2879. (f) Burdett, J. K.; Eisenstein, O.; Jackson, S. A. *Transition Metal Hydrides*; Dedieu, A., Ed.; VCH Publishers: New York, 1992; Chapter 5, p 149. (g) Lin, Z.; Hall, M. B. *J. Am. Chem. Soc.* **1992**, *114*, 6102. (h) Crow, J. S.; Backslay, G. B.; Hush, N. S. *J. Am. Chem. Soc.* **1994**, *116*, 5937. (i) Maseras, F.; Lledós, A.; Costas, M.; Poblet, J. M. *Organometallics* **1996**, *15*, 2947.

(12) Dapprich, S.; Frenking, G. *Angew. Chem. Int. Ed. Engl.* **1995**, *34*, 354. (b) Gelabert, R.; Moreno, M.; Lluch, J. M.; Lledós, A. *Organometallics* **1997**, *16*, 3805.

(13) Li, J.; Dickson, R. M.; Ziegler, T. *J. Am. Chem. Soc.* **1995**, *117*, 11482. (b) Li, J.; Ziegler, T. *Organometallics* **1996**, *15*, 3844. (c) Dapprich, S.; Frenking, G. *Organometallics* **1996**, *15*, 4547.

(14) Tomàs, J.; Lledós, A.; Jean, Y. *Organometallics* **1998**, *17*, 190.

(15) Frisch, M. J.; Trucks, G. W.; Schlegel, H. B.; Gill, P. M. W.; Johnson, B. G.; Robb, M. A.; Cheeseman, J. R.; Keith, T. A.; Petersson, G. A.; Montgomery, J. A.; Raghavachari, K.; Al-Laham, M. A.; Zakrzewski, V. G.; Ortiz, J. V.; Foresman, J. B.; Cioslowski, J.; Stefanov, B. B.; Nanayakkara, A.; Challacombe, M.; Peng, C. Y.; Ayala, P. Y.; Chen, W.; Wong, M. W.; Andres, J. L.; Replogle, E. S.; Gomperts, R.; Martin, R. L.; Fox, D. J.; Binkley, J. S.; Defrees, D. J.; Baker, J.; Stewart, J. P.; Head-Gordon, M.; Gonzalez, C.; Pople, J. A. *Gaussian 94*; Gaussian Inc.: Pittsburgh, PA, 1995.

(16) Parr, R. G.; Yang, W. *Density-Functional Theory of Atoms and Molecules*; Oxford University Press: Oxford, U.K., 1989.

(17) Lee, C.; Yang, W.; Parr, R. G. *Phys. Rev. B* **1988**, *37*, 785. (b) Becke, A. D. *J. Chem. Phys.* **1993**, *98*, 5648. (c) Stephens, P. J.; Devlin, F. J.; Chabalowski, C. F.; Frisch, M. J. *J. Phys. Chem.* **1994**, *98*, 11623.

(18) Hay, P. J.; Wadt, W. R. *J. Chem. Phys.* **1985**, *82*, 299.

(19) Hehre, W. J.; Ditchfield, R.; Pople, J. A. *J. Chem. Phys.* **1972**, *56*, 2257. (b) Hariharan, P. C.; Pople, J. A. *Theor. Chim. Acta* **1973**, *28*, 213. (c) Francl, M. M.; Pietro, W. J.; Hehre, W. J.; Binkley, J. S.; Gordon, M. S.; DeFrees, D. J.; Pople, J. A. *J. Chem. Phys.* **1982**, *77*, 3654.

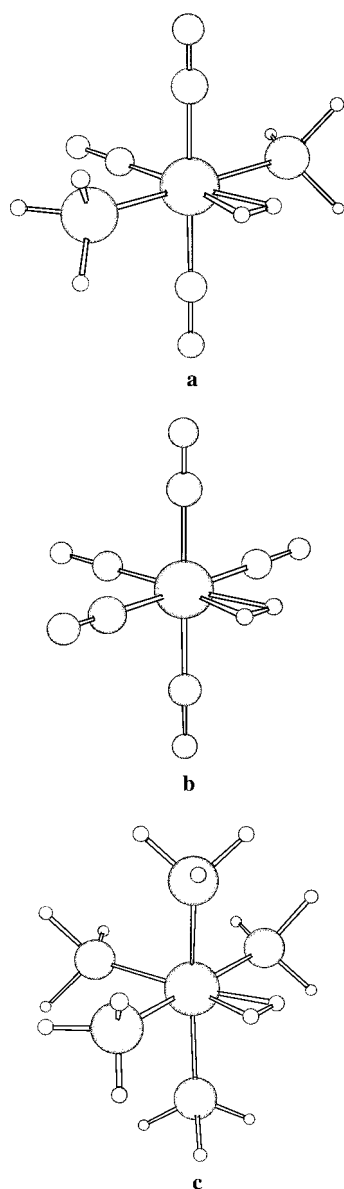
(20) Bartlett, R. J. *J. Phys. Chem.* **1989**, *93*, 1697. (b) Bartlett, R. J.; Watts, J. D.; Kucharski, S. A.; Noga, J. *Chem. Phys. Lett.* **1990**, *165*, 513.

(21) Bauschlicher, C. W., Jr.; Partridge, H. *J. Chem. Phys.* **1995**, *103*, 1788. (b) Mebel, A. M.; Morokuma, K.; Lin, M. C. *J. Chem. Phys.* **1995**, *103*, 7414.

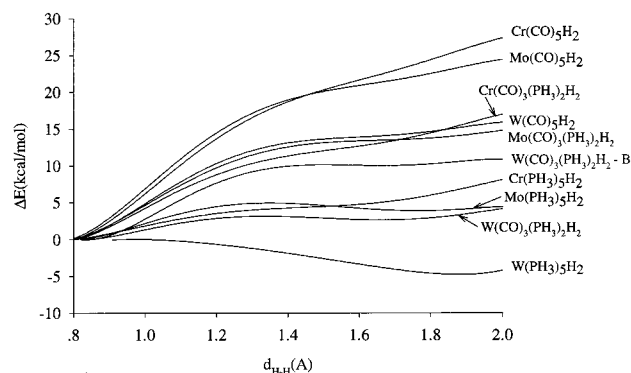
Table 1. Optimized Bond Lengths (Å) and H₂ Dissociation Energies (kcal/mol) for M(CO)_n(PR₃)_{5-n}(η²-H₂) Complexes

| | M–H | | | | H–H | | | | D _e | | | |
|---|-------------------|-------------------|-------------------|-------------------|-------------------|-------------------|-------------------|-------------------|-------------------|-------------------|-------------------|--|
| | calc ^a | calc ^b | calc ^c | expt | calc ^a | calc ^b | calc ^c | expt | calc ^a | calc ^b | calc ^c | expt |
| M(CO) ₃ (PH ₃) ₂ H ₂ | | | | | | | | | | | | |
| Cr | 1.782 | 1.857 | | | 0.808 | 0.822 | | 0.85 ^d | 16.9 | 21.3 | | 7.3 ± 0.1 ^{e,f} /6.8 ± 0.5 ^g |
| Mo | 1.965 | 1.897 | | | 0.804 | 0.848 | | 0.87 ^h | 17.1 | 19.2 | | 6.5 ± 0.2 ^{e,f} |
| W | 1.918 | 1.872 | | 1.89 ⁱ | 0.832 | 0.862 | | 0.82 ⁱ | 21.3 | 20.9 | | 9.4 ± 0.1 ^{e,f} |
| M(CO) ₅ H ₂ | | | | | | | | | | | | |
| Cr | 1.808 | | 1.745 | | 0.794 | | 0.814 | | 17.9 | | 19.8 | 15 ± 1.3 ^j |
| Mo | 2.006 | 1.899 | 1.959 | | 0.787 | 0.824 | 0.791 | | 15.7 | 19.6 | 16.6 | |
| W | 1.969 | | 1.918 | | 0.802 | | 0.810 | | 19.1 | | 19.8 | >16 ^j |
| M(PH ₃) ₅ H ₂ | | | | | | | | | | | | |
| Cr | 1.730 | | | | 0.829 | | | | 18.7 | | | |
| Mo | 1.854 | | | | 0.858 | | | | 23.5 | | | |
| W | 1.823 | | | | 0.911 | | | | 29.8 | | | |

^a This work. ^b DFT calculation from ref 13b. ^c MP2 calculation from ref 12a. ^d Solid-state NMR distance from ref 7. ^e Reference 23. ^f An agostic interaction is present on the M(CO)₃(PR₃)₂ metal fragments (R=Cyp, *i*-Pr).²⁴ ^g Reference 22. ^h Solid-state NMR distance from ref 6c. ⁱ Reference 3. ^j Reference 25.

**Figure 1.** Optimized structures of the dihydrogen molybdenum complexes Mo(CO)₃(PH₃)₂(H₂) (**1a**), Mo(CO)₅(H₂) (**1b**), and Mo(PH₃)₅(H₂) (**1c**).

Frenking et al. have found a nearly linear correlation between the calculated $D_e(\text{M}-\text{H}_2)$ energies and the $r(\text{H}-$

**Figure 2.** Energy profiles associated with the H–H bond breaking in the M(CO)_n(PH₃)_{5-n}(H₂) complexes (M = Cr, Mo, W; *n* = 0, 3, 5).

H) equilibrium values.^{13c} Our optimized geometrical parameters also reflect this trend. On the whole, the larger the binding energy, the longer the H–H distance and, for a given metal, the shorter the M–H distance.

Dihydrogen complexes have often been described as arrested forms along the reaction path in the oxidative addition process. Our results indicate that the largest binding energies are found for complexes in which the geometrical reorganization associated with this process (H–H lengthening and M–H shortening) is the most advanced. These complexes with strong M–H₂ bonds are actually those for which the whole oxidative addition process is the easiest.

Dihydrogen Addition

The energy profiles associated with the H–H bond breaking were calculated for the nine complexes (Figure 2). For each complex, the H–H distance was varied from 0.8 to 2.0 Å by steps of 0.2 Å, all the other geometrical parameters being optimized at the B3LYP level at each fixed H–H distance. Single-point energy-only calculations were performed at the CCSD(T) level on all the optimized structures. The potential energy curve for the W(CO)₃(PH₃)₂(H₂) complex, already presented in our previous work,¹⁴ is also included in Figure 2 for comparative purpose.

The tungsten complexes actually provide a very nice illustration of the three possible cases one may encounter for the dihydrogen vs dihydride problem. In the

pentacarbonyl complex, the H–H breaking is an energy-costing reaction (14.6 kcal/mol to stretch the H–H bond to 1.8 Å), and there is no minimum associated with a *cis*-dihydride structure. On the contrary, the dihydride form is lower in energy in the pentaphosphine complex, in agreement with the experimental data,^{9a,10b} and no stable structure is associated with the dihydrogen form (the rather elongated minimum found at the B3LYP level disappears at the CCSD(T) level). However, it must be stressed that the energy profile associated with the breaking of the H–H bond in this system is very flat, pointing out that the *cis*- $WH_2(PH_3)_5$ might not be the experimental structure adopted for the $WH_2(PR_3)_5$ (R = Me, OMe) complexes (we will return to this point in the next section). Finally, an intermediate situation is found for the Kubas complex, with the two forms close in energy and a very low barrier for the oxidative addition. As a matter of fact, dihydrogen and dihydride complexes are known to coexist in solution.⁶

To check the role of the orientation of the dihydrogen addition in the Kubas complex, we have also calculated the energy profile for the addition in the plane of the carbonyl ligands, giving rise to a *cis*-dihydride pentagonal bipyramidal structure with two axial phosphine ligands (curve $W(CO)_3(PH_3)_2(H_2)$ -B in Figure 2). In this case, the oxidative addition starts from a conformation with the dihydrogen rotated by 90° with respect to the minimum. The most striking fact is that the oxidative addition is much more difficult in the later case, and as the d donating orbital is stabilized by three π^*_{CO} orbitals (instead of only one in the actual structure), the curve is very similar to the tungsten pentacarbonyl one.

For a given set of ligands, the oxidative addition process is remarkably easier for the tungsten than for the molybdenum and chromium complexes, a very similar energy cost being found for the two latter metals. Energy profiles for $M(CO)_3(PH_3)_2(H_2)$ complexes are alike with the observation of a dihydrogen/dihydride equilibrium for M = W and the nondetection of the corresponding Mo and Cr dihydrides. Same trends for the effect of the metal and the ancillary ligands are found in $M(CO)_5(H_2)$ and $M(PH_3)_5(H_2)$ systems. From these energy profiles, the fact that a group 6 transition metal pentacarbonyl dihydride has never been isolated can be easily understood.

In agreement with the experimental data,^{10b} the results for the pentaphosphine complexes clearly show that hydrogen dissociation (reductive elimination) in $MoH_2(PH_3)_5$ is easier than in the tungsten analogue. The energy profiles also indicate that whereas the dihydrogen form is not stable in the W complex, this structure is thermodynamically favored over the *cis*-dihydride in the Cr and Mo complexes. Our calculations thus suggest that a dihydrogen/dihydride equilibrium could take place in these complexes, although it has not yet been detected. Finally, a *cis* structure for this dihydride is not expected since there is essentially no barrier for the return to the dihydrogen. As a matter of fact, the only group 6 dihydride characterized by X-ray diffraction ($MoH_2(PMe_3)_5$) does not adopt a *cis* arrangement for the hydrides.^{9b}

Structure and Stability of the Dihydride Form

The energy profiles given in Figure 2 are associated with the simple cleavage of the H–H bond in a dihy-

Table 2. Optimized Geometrical Parameters Associated with the PB1 and PB2 Structures of the $MoH_2(PH_3)_5$ Complex^a

| | PB1 | PB2 | expt ^b |
|----------|--------------------|-------|-------------------|
| Mo–P4 | 2.425 | 2.421 | 2.424(3) |
| Mo–P5 | 2.420 | 2.417 | 2.426(3) |
| Mo–P6 | 2.450 | 2.422 | 2.403(3) |
| Mo–P7 | 2.450 | 2.453 | 2.478(3) |
| Mo–P8 | 2.491 | 2.445 | 2.469(3) |
| Mo–H2 | 1.740 | 1.768 | 1.67(3) |
| Mo–H3 | 1.740 | 1.754 | 1.69(4) |
| H2–H3 | 1.800 ^c | 3.307 | |
| P6–Mo–H2 | 126.6 | 67.0 | 66(2) |
| H2–Mo–P7 | 64.3 | 66.7 | 66(2) |
| P7–Mo–P8 | 84.6 | 88.9 | 99.2(1) |
| P8–Mo–H3 | 148.8 | 63.8 | 59(1) |
| H3–Mo–P6 | 64.3 | 72.8 | 70(1) |
| P6–Mo–P5 | 89.2 | 88.5 | 90.9(1) |
| P6–Mo–P4 | 92.2 | 88.1 | 87.9(1) |

^a For the atom numbering, see Figure 3. Distances are given in angstroms and angles in degrees. ^b X-ray data of the $MoH_2(PMe_3)_5$ complex.^{9b} ^c Fixed.

drogen-like structure. This mechanism leads to a pentagonal bipyramidal structure in which the hydrides are *cis* to each other (**PB1**). Although it is likely to be the first step for the oxidative addition process, this structure is not necessarily the most stable for the dihydride form, as we demonstrated in our previous study on $W(CO)_3(PH_3)_2H_2$: the actual structure is a pentagonal bipyramid with two equatorial hydrides separated by a phosphine ligand (**PB2**).¹⁴ On the other hand, the X-ray study of $MoH_2(PMe_3)_5$ has revealed the same type of structure.^{9b}

Our previous study on the dihydride form for the Kubas complex pointed out a small energy difference between **PB1** and **PB2** structures. According to the qualitative rules for the substituent site preferences in d^4 pentagonal bipyramid complexes,²⁶ two structures that differ only by the position of two σ -donor ligands in the equatorial plane are essentially identical from an electronic point of view. Therefore, in $M(CO)_5H_2$ complexes, where the *cis*-dihydride **PB1** is a high-energy species, the **PB2** structures were not studied. The remaining six **PB2** structures were optimized and found to be stable with respect to the conversion toward the dihydrogen complex. This fact contrasts with the unstability of **PB1** structures, for which only a chemically significant minimum was found in the $WH_2(PH_3)_5$ complex.

The energies of the dihydride structures (given with respect to that of the dihydrogen complex) are reported in Table 3. Although we have not found *cis*-dihydride (**PB1**) minima in most of the systems, we calculated the energy of such structures at a fixed distance of 1.8 Å, the other geometrical parameters being optimized. Energies of **PB1** will give us an idea of the energy cost

(22) Bender, B. R.; Kubas, G. J.; Llewellyn, H. J.; Swanson, B. I.; Eckert, J.; Capps, K. B.; Hoff, C. D. *J. Am. Chem. Soc.* **1997**, *119*, 9179.

(23) Gonzalez, A. A.; Zhang, K.; Nolan, S. P.; Lopez de la Vega, R.; Mukerjee, S. L.; Hoff, C. D.; Kubas, G. J. *Organometallics* **1988**, *7*, 2429. (b) Gonzalez, A. A.; Hoff, C. D. *Inorg. Chem.* **1989**, *28*, 4295.

(24) Wasserman, H. J.; Kubas, G. J.; Ryan, R. R. *J. Am. Chem. Soc.* **1986**, *108*, 2294.

(25) Ishikawa, Y.-I.; Hackett, P. A.; Rayner, D. M. *J. Phys. Chem.* **1989**, *93*, 652. (b) Wells, J. R.; House, E.; Weitz, E. *J. Phys. Chem.* **1994**, *98*, 8343.

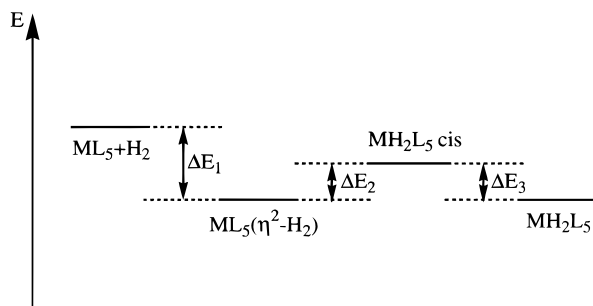
(26) Hoffmann, R.; Beier, B. F.; Muetterties, E. L.; Rossi, A. R. *Inorg. Chem.* **1977**, *16*, 511.

Table 3. Relative Energies (kcal/mol) of the Dihydride Structures with Respect to the Dihydrogen Form^a

| | PB1 | PB2 |
|--|------|------|
| CrH ₂ (CO) ₅ | 24.3 | |
| MoH ₂ (CO) ₅ | 22.5 | |
| WH ₂ (CO) ₅ | 14.6 | |
| CrH ₂ (CO) ₃ (PH ₃) ₂ | 14.4 | 11.5 |
| MoH ₂ (CO) ₃ (PH ₃) ₂ | 13.8 | 12.6 |
| WH ₂ (CO) ₃ (PH ₃) ₂ | 3.9 | 2.3 |
| CrH ₂ (PH ₃) ₅ | 6.0 | 1.5 |
| MoH ₂ (PH ₃) ₅ | 2.9 | 2.2 |
| WH ₂ (PH ₃) ₅ | -4.7 | -5.7 |

^a The relative energies are calculated at the CCSD(T) level.

Scheme 1

**Table 4. Thermodynamics of the Whole Dihydrogen Oxidative Addition Process (Scheme 1)^{a,b}**

| | ΔE_1 | ΔE_2 | ΔE_3 | ΔE_{total} |
|--|--------------|--------------|--------------|---------------------------|
| Cr(CO) ₅ H ₂ | -17.9 | 24.3 | | |
| Mo(CO) ₅ H ₂ | -15.7 | 22.5 | | |
| W(CO) ₅ H ₂ | -19.1 | 14.6 | | |
| Cr(CO) ₃ (PH ₃) ₂ H ₂ | -16.9 | 14.4 | -2.9 | -5.4 |
| Mo(CO) ₃ (PH ₃) ₂ H ₂ | -17.1 | 13.8 | -1.2 | -4.5 |
| W(CO) ₃ (PH ₃) ₂ H ₂ | -21.3 | 3.9 | -1.6 | -19.0 |
| Cr(PH ₃) ₅ | -18.7 | 6.0 | -3.5 | -16.2 |
| Mo(PH ₃) ₅ | -23.5 | 2.9 | -0.7 | -21.3 |
| W(PH ₃) ₅ | -29.8 | -4.7 | -1.0 | -35.5 |

^a The energies have been calculated at the CCSD(T) level. For ΔE_1 , energies with respect to the separated ML₅ + H₂ fragments at their equilibrium geometries. ^b Energies in kcal/mol.

of the H–H bond-breaking process. It can be seen from Table 3 that, in all cases, the energies of **PB2** structures are a bit lower than those of the **PB1** (*cis*) structures, only slight changes resulting for the energy difference between the dihydrogen and the dihydride forms. These results strengthen the proposal that the dihydrogen form is thermodynamically accessible in the M(PR₃)₂H₂ (M = Cr, Mo) systems and might be detected.

The Whole Process for Dihydrogen Addition

It is now possible to discuss the thermodynamics of the whole oxidative process which, starting from the ML₅ and H₂ separated fragments, leads to a stable **PB2** dihydride (Scheme 1).

Except for the M(CO)₅H₂ systems, where the process is ended at the dihydrogen complex, the reaction ML₅ + H₂ → MH₂L₅ is always thermodynamically favorable ($\Delta E_{\text{tot}} < 0$, Table 4). However, the H–H bond breaking leading to the *cis*-dihydride is thermodynamically favored only for the W(PH₃)₅H₂ system. A common feature of the complexes for which the dihydride is energetically close to the dihydrogen is that a geometrical rearrangement of a **PB1** into a **PB2** structure

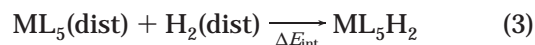
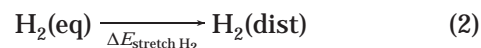
leads to a more stable dihydride. Variable-temperature NMR experiments have given an estimate of 8 kcal/mol for this rearrangement in CrH₂[P(OMe)₃]₅.^{10c}

The thermodynamic results and the energy profiles for the oxidative addition allow us now to classify the nine complexes under study in three groups: (i) Dihydrogen only; M(CO)₅H₂ (M = Cr, Mo, W) and M(CO)₃-(PH₃)₂H₂ (M = Cr, Mo); (ii) equilibrium between dihydrogen and **PB2** dihydride; W(CO)₃(PH₃)₂H₂, M(PH₃)₅H₂ (M = Cr, Mo); (iii) dihydride only; W(PH₃)₅H₂. In this case, both **PB1** and **PB2** dihydrides might be stable.

In the following, this different behavior will be related to physical properties of the ML₅ fragments and to the energetics of the metal–hydrogen bond.

Factors Governing the Energy Profile for the Dihydrogen Addition

Starting from the isolated ML₅ and H₂ fragments in their equilibrium geometries, the relative energy of a given structure can be decomposed into three terms associated with (i) the distortion of the ML₅ fragment, (ii) the stretching of H₂, and (iii) the interaction between the distorted ML₅ and the elongated H₂ fragments.



At each point of the energetic profile the variation in the total energy can be obtained by adding the three contributions, two destabilizing ($\Delta E_{\text{dist ML}_5}$ and $\Delta E_{\text{stretch H}_2}$) and one stabilizing (ΔE_{int}) (eq 4).

$$\Delta E_{\text{tot}} = \Delta E_{\text{dist ML}_5} + \Delta E_{\text{stretch H}_2} + \Delta E_{\text{int}} \quad (4)$$

This energy decomposition was performed at the B3LYP level for the nine M(CO)_n(PH₃)_{5-n}H₂ (M = Cr, Mo, W; n = 0, 3, 5) systems. Figure 4 displays the variation of the three terms in the Kubas complex.

The energy change associated with the distortion of the ML₅ fragment being small, the flat energy profile found for ΔE_{tot} results from the compensation of two large terms ($\Delta E_{\text{stretch H}_2}$ and ΔE_{int}). The same behavior in the $\Delta E_{\text{dist ML}_5}$ was found in all the other systems. Since the $\Delta E_{\text{stretch H}_2}$ curve is the same in all cases, the form of a given energy profile is governed by the ΔE_{int} term: depending on the slope of the ΔE_{int} curve, the dihydrogen, the dihydride or an equilibrium between the two isomers is found. Variations of the ΔE_{int} as a function of the H–H distance for the tungsten complexes and for the M(CO)₃(PH₃)₂H₂ complexes are depicted in Figures 5 and 6, respectively.

The curves show how the small energy differences in the dihydrogen region (~0.8 Å) are enlarged with increasing $d_{\text{H-H}}$, leading to large energy differences in the dihydride region (~1.8 Å). Note also the very similar shape of the curves for the chromium and molybdenum complexes (Figure 6).

Let us now analyze in more detail the ΔE_{int} term in both the dihydrogen and dihydride forms. In the former, it roughly corresponds to the energy of the

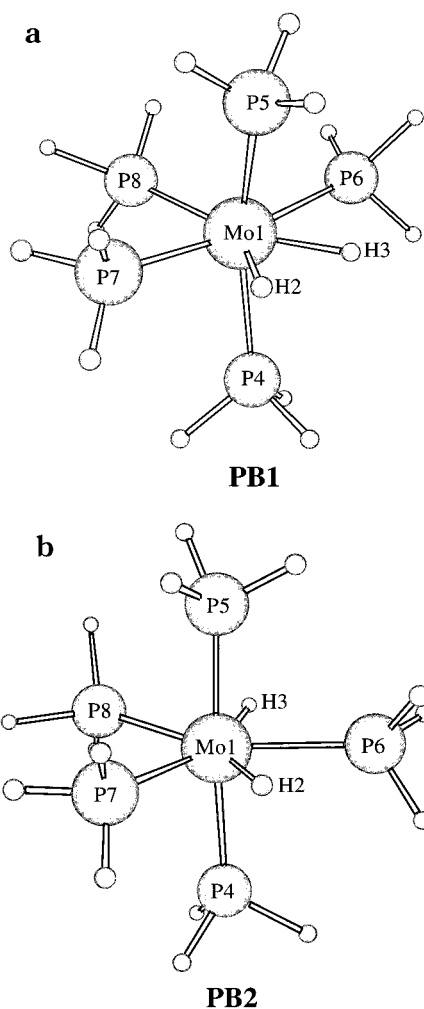


Figure 3. Optimized structures of the $MoH_2(PH_3)_5$ dihydride: (a) **PB1**, (b) **PB2**.

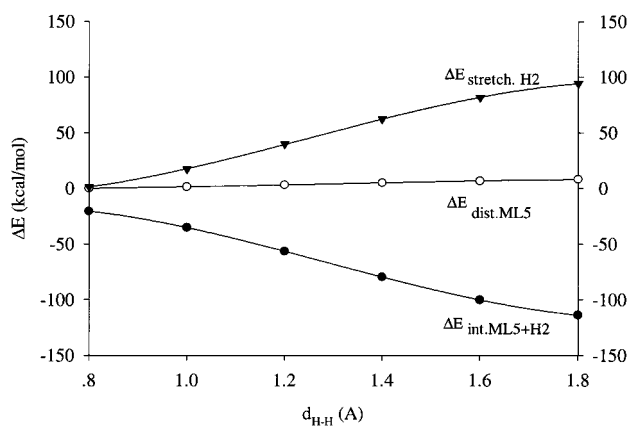


Figure 4. Energy decomposition as a function of the H–H distance for the $W(CO)_3(PH_3)_2H_2$ complex.

$M-H_2$ bond ($D_e(M-H_2)$). The way the nature of the metal and the ancillary ligands influence its value has been already discussed in the first section. The situation is a bit more complicated in the dihydride region, since the formation of two $M-H$ bonds is accompanied by a strong electronic reorganization. The $M-H$ bond formation can actually be decomposed in a two-step process: (i) promotion of one electron from a d_π to a d_σ orbital in the ML_5 fragment, leading to an excited triplet state: the metal fragment with two unpaired electrons

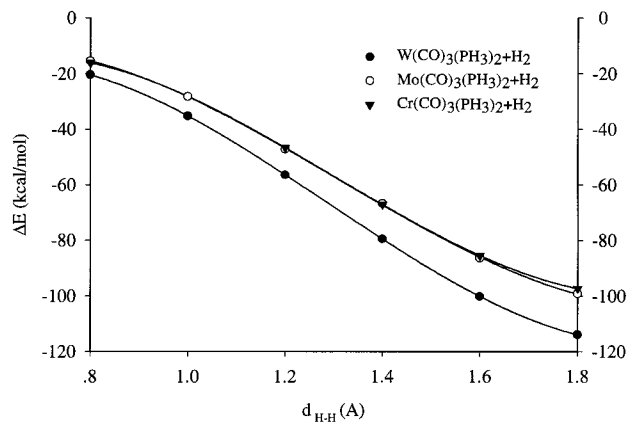


Figure 5. Variation of the ΔE_{int} term as a function of the H–H distance for the $W(CO)_n(PH_3)_{5-n}H_2$ systems ($n = 0, 3, 5$).

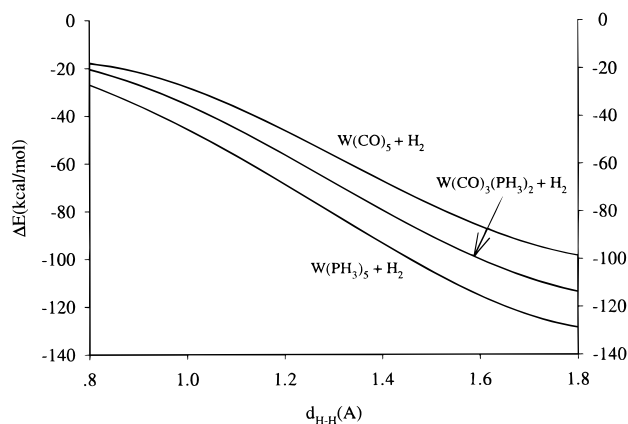


Figure 6. Variation of the ΔE_{int} term as a function of the H–H distance for the $M(CO)_3(PH_3)_2H_2$ systems ($M = Cr, Mo, W$).

is now in the optimal situation to bind two more ligands; (ii) formation of the two $M-H$ bonds with the essentially noninteracting hydrogen atoms of the elongated H_2 fragment.

Therefore, the ΔE_{int} contribution in the dihydride region depends not only on the energetics of the $M-H$ bond formation, as might have been expected, but also on the singlet/triplet separation in the ML_5 fragment. Hay has already discussed from Hartree–Fock calculations the importance of $d_\pi \rightarrow d_\sigma$ promotion energies in WL_5 fragments for the dihydrogen vs dihydride problem.^{11b} On the other hand, it has been shown recently by MP2 calculations that the singlet/triplet energy gap in $CpM(PH_3)(CH_3)^+$ ($M = Rh, Ir$) species can be a useful guide to predict its reactivity for oxidative addition reactions.²⁷

According to the above analysis, the dihydride structure should be favored (large $|\Delta E_{int}|$) by a small singlet/triplet separation ($\Delta E_{S/T}$) and by large $M-H$ binding energies ($D_e(M-H)$). The $\Delta E_{S/T}$ and $D_e(M-H)$ terms were calculated at the CCSD(T)//B3LYP level for the nine complexes under study. For the former, the excitation involves the orbitals required for the further formation of the $M-H$ bonds. The $M-H$ bond energies were calculated as the energy difference between the ML_5 fragment optimized in its triplet state plus two

(27) Su, M.-D.; Chu, S.-Y. *J. Am. Chem. Soc.* **1997**, *119*, 5373.

Table 5. Singlet/Triplet Energetic Separation, M–H and M–H₂ Bond Energies, and Dihydrate/Dihydrogen Energetic Difference (kcal/mol)^a

| | $\Delta E_{S/T}$ | $D_e(M-H)$ | $D_e(M-H_2)$ | $\Delta E_{\text{dihydrate/dihydrogen}}$ |
|---|------------------|------------|--------------|--|
| Cr(CO) ₃ (PH ₃) ₂ | 14.1 | 61.2 | 16.9 | 14.4 |
| Mo(CO) ₃ (PH ₃) ₂ | 30.1 | 69.6 | 17.1 | 13.8 |
| W(CO) ₃ (PH ₃) ₂ | 23.7 | 73.5 | 21.3 | 3.9 |
| W(CO) ₃ (PH ₃) ₂ -B | 32.2 | 73.4 | 20.3 | 7.3 |
| Cr(CO) ₅ | 25.1 | 62.2 | 17.9 | 24.3 |
| Mo(CO) ₅ | 40.0 | 68.0 | 15.7 | 22.5 |
| W(CO) ₅ | 30.8 | 70.6 | 19.1 | 14.6 |
| Cr(PH ₃) ₅ | 5.7 | 62.1 | 18.7 | 6.0 |
| Mo(PH ₃) ₅ | 23.6 | 75.0 | 23.5 | 2.9 |
| W(PH ₃) ₅ | 20.0 | 79.5 | 29.8 | -4.7 |

hydrogen atoms and the *cis*-dihydrate complex (**PB1**). The results are collected in Table 5 together with the $D_e(M-H_2)$ values for the dihydrogen complex and the energy difference between dihydrogen and *cis*-dihydrate structures ($\Delta E_{\text{dihydrate/dihydrogen}}$).

The ligand effects in the dihydrogen addition are well accounted by the $\Delta E_{S/T}$ term. For each metal, the largest $\Delta E_{S/T}$ is found for the pentacarbonyl complex, and the smallest for the pentaphosphine one. Let us note that the singlet/triplet separation is equivalent to the HOMO/LUMO gap usually considered (as are state vs correlation diagrams).

As a matter of fact, the stabilization of the d_{π} orbital by bonding interaction with the π^*_{CO} orbital increases the singlet/triplet energy excitation. These results agree with the easier dihydrogen addition in $M(\text{PH}_3)_5\text{H}_2$ systems where there is no stabilization of the d_{π} orbital. The changes in $\Delta E_{S/T}$ also explain the favored orientation of the addition in the Kubas complex. The B-orientation is associated with the 3B_2 triplet state of the $W(\text{CO})_3(\text{PH}_3)_2$ metal fragment, which is lying 8.5 kcal/mol above the 3B_1 triplet state, suitable for the preferred orientation.

However, the influence of the metal cannot be interpreted from $\Delta E_{S/T}$ changes, since the lowest values are found for the chromium compounds. The $D_e(M-H)$ term has to be taken into account to understand the different behavior of the three group 6 metals with a given set of ancillary ligands. The computed values of $D_e(M-H)$ (Table 5) are in the range of the experimental group 6 M–H bond enthalpies.²⁸ For instance, $D_e(M-H)$ values of 61.7 ± 0.7 , 65.3 ± 2.2 , and 81.1 ± 1.2 kcal/mol have been determined in $M(\text{Cp})(\text{CO})_3\text{H}$ complexes for $M = \text{Cr}, \text{Mo},$ and W , respectively. Our $D_e(W-H)$ for the $\text{WH}_2(\text{CO})_3(\text{PH}_3)_2$ (73.5 kcal/mol) is not far from the estimated average W–H bond energy of 65 ± 6 kcal/mol for the dihydrate isomer of $W(\text{PR}_3)_2(\text{CO})_3\text{H}_2$.²⁹ In the chromium complexes, the computed M–H bond energy was found to be almost independent of the nature of the ancillary ligands and significantly smaller than in the Mo or W complexes. In the latter, the strongest M–H bonds were found for the pentaphosphine compounds, the bond energy decreasing with increasing number of carbonyl ligands.

(28) Martinho Simões, J. A.; Beauchamp, J. L. *Chem. Rev.* **1990**, *90*, 629, and references therein.

(29) Gonzalez, A. A.; Zhang, K.; Mujerke, S. L.; Hoff, C. D.; Khalsa, G. R.; Kubas, G. J. In *Bonding Energetics in Organometallic Compounds*; ACS Symposium Series 428; Marks, T. J., Ed.; American Chemical Society: Washington, DC, 1990.

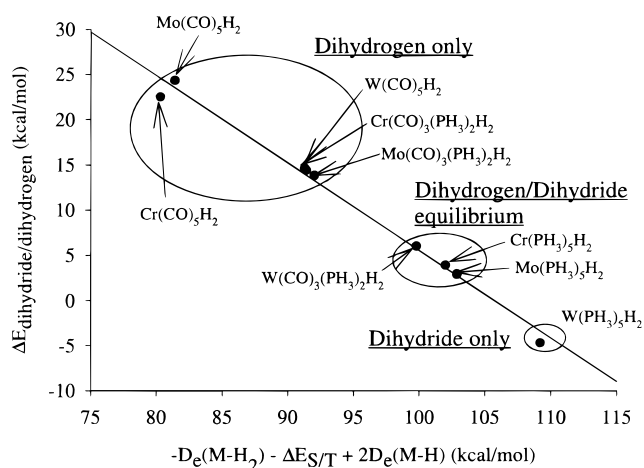
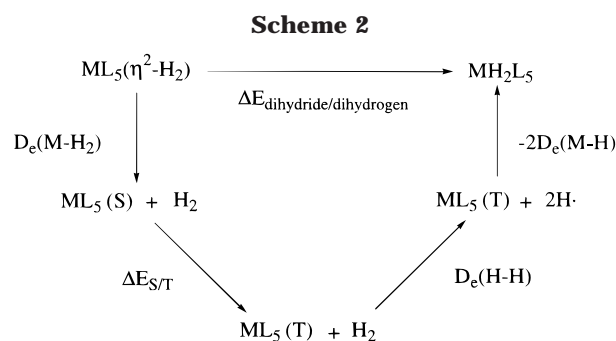


Figure 7. Plot of the $\Delta E_{\text{dihydrate/dihydrogen}}$ vs $-D_e(M-H_2) - (\Delta E_{S/T} + 2D_e(M-H))$.



Combining the $\Delta E_{S/T}$ and $D_e(M-H)$ values allows a rationalization of the evolution of the ΔE_{int} term, which has been shown to be crucial for the feasibility of the oxidative addition reaction. For a given set of ligands, the smallest values of both $\Delta E_{S/T}$ and $D_e(M-H)$ are found in the Cr complexes. In the Mo analogues, the M–H bonds are stronger, which is favorable for the dihydrate structure, but $\Delta E_{S/T}$ is larger, which is unfavorable. Therefore, the similar behavior of Cr and Mo complexes in the dihydrogen oxidative addition process comes from the compensation of two factors working in opposite direction. Comparison between W and Mo shows that, for a given set of ligands, the M–H bonds are stronger and the singlet/triplet separation smaller in W than in Mo complexes. Both factors thus make the oxidative addition easier in W than in Mo and Cr complexes.

Dihydrate/Dihydrogen Energy Difference Derived from a Thermodynamic Cycle

It is possible to construct a thermodynamical cycle relating the dihydrogen and the dihydrate forms which involves the energetic terms defined above (Scheme 2). This cycle can be described as follows: (i) starting from the dihydrogen complex, the departure of H_2 leads to the isolated low-spin ML_5 and H_2 fragments ($D_e(M-H_2)$); (ii) singlet/triplet excitation is performed in the ML_5 fragment ($\Delta E_{S/T}$); (iii) the H–H bond is broken ($D_e(H-H)$); (iv) finally, the two M–H bonds are formed, leading to the dihydrate structure ($-2D_e(M-H)$). It follows that the energy difference between the dihydrate

and the dihydrogen form obeys the following relation (eq 5):

$$\Delta E_{\text{dihydride/dihydrogen}} = D_e(\text{M}-\text{H}_2) + \Delta E_{\text{S/T}} + D_e(\text{H}-\text{H}) - 2D_e(\text{M}-\text{H}) \quad (5)$$

Therefore, plotting $\Delta E_{\text{dihydride/dihydrogen}}$ (y) as a function of $-D_e(\text{M}-\text{H}_2) - \Delta E_{\text{S/T}} + 2D_e(\text{M}-\text{H})$ (x) should lead to a straight line with a slope equal to -1 and passing by the point $(D_e(\text{H}-\text{H}), 0)$, i.e., (104.2 kcal/mol, 0). This is actually a very demanding test for our calculations, since three computed values, $D_e(\text{M}-\text{H}_2)$, $\Delta E_{\text{S/T}}$, and $D_e(\text{M}-\text{H})$, for each of the nine complexes are involved. The result given in Figure 7 shows that the nine points are almost exactly located on a straight line with a slope of -0.97 . Furthermore, the point for which the dihydride–dihydrogen energy difference vanishes corresponds to $x = 105.7$ kcal/mol, a value almost exactly equal to $D_e(\text{H}-\text{H})$.

The different behavior of the various complexes in front of the dihydrogen addition clearly appears on this straight line correlation. For the five complexes on the left-hand side, the addition is arrested at the dihydrogen structure, while for the three complexes in the middle of the line an equilibrium between the dihydrogen and the dihydride forms can take place. For the single complex of the right-hand side, the oxidative addition is completed and only the dihydride form is observed. Note that a clear distinction is found between the three regions associated with the three possible behaviors recalled in the Introduction for the dihydrogen addition. What is remarkable for the series of complexes under

study is that these three regions are “populated” by one or several systems.

It is noteworthy that the linear relationship (eq 5) derived from Scheme 2 does not depend on the particular nature of the metal fragment (ML_5 in the present study). The same relation applies to the dihydrogen addition on any ML_n species. The $\Delta E_{\text{dihydride/dihydrogen}}$ values should thus always lie on the very same line in one of the three regions recognized above depending on the ease of the oxidative addition.

Finally, a thermodynamical cycle similar to that depicted in Scheme 2 can be constructed for the interaction and eventual breaking of any $X-Y$ bond at a metal center. Again, a linear correlation should be found, the straight line being parallel to that given in Figure 7. As a matter of fact, the zero value for $\Delta E(\text{Y}-\text{M}-\text{X}/\text{M}-\text{XY})$ would now correspond to the dissociation energy of the $X-Y$ bond instead of that of $\text{H}-\text{H}$.

Acknowledgment. Y.J. is grateful to the IBERDROLA Company for an invitation as Visiting Professor at the Universitat Autònoma de Barcelona. J.T. and A.L. acknowledge financial support from the D.G.E.S. of Spain Project No. PB95-0639-C02-01. J.T. acknowledges the “Direcció General de Recerca de la Generalitat de Catalunya” for a Grant. The use of computational facilities of the Centre de Supercomputació i Comunicacions de Catalunya is gratefully appreciated as well. Support is also acknowledged from the “Acció Integrada Hispano-Francesa” (Grant No. 96034/236).

OM980308N